This is the accepted manuscript version of the article "Daugas, J M et al, Physical Review C, **104**, 024321. https://doi.org/10.1103/PhysRevC.104.024321".

# Magnetic moment of the $11/2^-$ isomeric state in $^{99}$Mo and neutron spin $g$ factor quenching in A$\sim$100 nuclei

J. M. Daugas,[1] B. Rosse,[1] D. L. Balabanski,[2] D. Bucurescu,[3,4] S. Kisyov,[3] P. H. Regan,[5,6] L. Gaudefroy,[1,7] G. Georgiev,[8] K. Gladnishki,[9] V. Méot,[1,7] P. Morel,[1,7] S. Pietri,[10] O. Roig,[1,7] and G. S. Simpson[11]

[1] *CEA, DAM, DIF, 91297 Arpajon cedex, France*
[2] *Extreme Light Infrastructure - Nuclear Physics (ELI-NP), Horia Hulubei National Institute for R&D in Physics and Nuclear Engineering (IFIN-HH), 077125 Bucharest-Măgurele, Romania*
[3] *Horia Hulubei National Institute for R&D in Physics and Nuclear Engineering (IFIN-HH), 077125 Bucharest- Măgurele, Romania*
[4] *Center for Advanced Studies in Physics of the Romanian Academy, 13, Calea 13 Septembrie, Bucharest, Romania*
[5] *Department of Physics, University of Surrey, Guildford, GU2 7XH, United Kingdom*
[6] *National Physical Laboratory, Teddington, Middlesex TW11 0LW, United Kingdom*
[7] *Univ Paris Saclay, CEA, Lab Mat Condit Extremes, Bruyères Le Châtel, France*
[8] *Université Paris-Saclay, CNRS/IN2P3, IJCLab, 91405 Orsay, France*
[9] *Faculty of Physics, St. Kliment Ohridski University of Sofia, 1164 Sofia, Bulgaria*
[10] *GSI Helmholtzzentrum fur Schwerionenforschung GmbH, Planckstr. 1, 64291 Darmstadt, Germany*
[11] *LPSC, CNRS/IN2P3, Université Joseph Fourier Grenoble 1, INPG, 38026 Grenoble Cedex, France*

(Dated: January 20, 2021)

The gyromagnetic factor of the low-lying $E_x = 684.10(19)$ keV isomeric state of the nucleus $^{99}$Mo was measured using the Time Dependent Perturbed Angular Distribution technique. This level is assigned a spin and parity of $J^\pi = 11/2^-$, with a half-life of $T_{1/2} = 742(13)$ ns. The state of interest was populated and spin-aligned via a single-neutron tranfer on an highly enriched $^{98}$Mo target. A magnetic moment $\mu_{\mathrm{exp.}} = -0.627(20)\mu_{\mathrm{N}}$ was obtained. This result is far from the Schmidt value expected for a pure single-particle $\nu h_{11/2}$ state. A comparison of experimental spectroscopic properties of this nucleus is made with results of multi-shell Interacting Boson-Fermion Model IBFM-1 calculations. In this approach, the $J^\pi = 11/2^-$ isomeric state in $^{99}$Mo has a pure $\nu h_{11/2}$ configuration. Its magnetic moment, as well that of other two excited states could be reasonably well reproduced only by reducing the free neutron spin $g$ factor with a quenching factor of 0.45. This low value is not appropriate only for this case, similar values for the quenching factor being also required in order to describe magnetic moments in other nuclei from the same mass region.

PACS numbers: 21.10.Ky, 21.60.-n, 23.20.En, 23.35.+g, 25.45.Hi

## I. INTRODUCTION

The nuclear magnetic dipole moment is a highly sensitive probe of the single-particle properties of the nuclear wave function. The gyromagnetic factor ($g$ factor) of a state is the ratio of its magnetic moment ($\mu$) to spin ($J$), $g = \mu/J$. The knowledge of the g factor of a state can allow confirmations of spin and parity assignments and provide information on the valence-orbit occupancy. Because magnetic moments only depend on the wave function of the studied nuclear state, and not on the transition between states as for transition probabilities or spectroscopic factors, their knowledge is a good test for nuclear models.

Magnetic moments for the neutron $h_{11/2}$ orbital at the closed proton $Z = 50$ shell [1] display a smooth variation along the Sn isotopes with an extracted $g$ factor around $g = -0.25$. This result is in perfect agreement with the effective Schmidt value [2] applying a common quenching factor of 0.7 to the free single particle $g$ factor of the spin motion, $g_{\mathrm{s}}^{\mathrm{eff}} = 0.7\ g_{\mathrm{s}}^{\mathrm{free}}$, reflecting the effect of the core polarization and the meson exchange current. Measurements of the $g$ factors for the same orbital below the $Z = 50$ shell have been done for many isotopes along the Cd, $Z = 48$, chain, above the neutron number $N = 59$ [1, 3]. Experimental values are still displaying a smoth variation. For both cases, the smooth variation of the occupation numbers has been attributed to strong pairing correlations [4]. The $g$ factors for the Cd isotopes are found to be about 25 % below the Sn ones, around $g = -0.20$. Here, one has to reduce the quenching factor down to 0.6 to reproduce the measured g factors. It is interesting to note that the same feature was observed by reproducing the experimentally reduced transition probability $B(M2)$ values between the $\nu h_{11/2}$ and $\nu g_{7/2}$ configurations in $^{95-99}$Mo, $^{99}$Ru and $^{101}$Pd which were satisfactorily described within the quasiparticle-phonon model using $g_{\mathrm{s}}^{\mathrm{eff}} = 0.6\ g_{\mathrm{s}}^{\mathrm{free}}$ [5]. Thus, the importance of the core polarization depends on the filling of the proton shell.

Farther away from $Z = 50$ only one $g$ factor was measured so far for the $J^\pi = 11/2^-$ state in the $^{103}$Pd isotope with $Z = 46$ and $N = 57$, where a value of $g = -0.19(1)$ [1] was reported. The uncertainty of this result does not allow us to judge the evolution of the $g$ factor when going from 2 to 4 proton holes away from a closed shell. Therefore, it is important to investigate the $g$ factor of the $\nu h_{11/2}$ orbital for isotopes below Cd and Pd in order to get information on the evolution of the wave function, of the quenching factor and the role of the core polarization when going away from closed proton shell.

The $Z = 42$ Molybdenum isotopes, with mass number around 100, lie in a transitional region where different degrees of freedom influence the evolution of nuclear structure. The work of P. H. Regan and collaborators [6] reveals the interplay between rotational motion and vibrations in the Mo nuclei. The $\nu h_{11/2}$ intruder orbital defines the collective properties in this mass region. Regular sequences of $\gamma$ rays which are built on the $\nu h_{11/2}$ orbital have been observed throughout the region [7–12]. In $^{99}$Mo, a second microsecond isomeric level, located above the $T_{1/2} = 15.5$ $\mu$s, $J^\pi = 5/2^+$, $E_x = 97.785$ keV one [13], at an excitation energy of $E_x = 684.10$ keV was first observed by the work of Ref. [14]. This second isomeric state will be noted in the following as $^{99\mathrm{m}2}$Mo. A spin and parity assignment was reported to be $J^\pi = 11/2^-$ [14, 15], with an expected pure $\nu h_{11/2}$ configuration. The $^{99\mathrm{m}2}$Mo has a weakly prolate shape and was identified as the head of the decoupled band associated with the population of the low-K components of the unique-parity $\nu h_{11/2}$ orbital [9, 15]. This isomer decays via the 448.6 keV $M2$ transition to the $J^\pi = 7/2^+$ level with a mainly $\nu g_{7/2}$ configuration with a reduced transition rate of $B(M2) = 0.103(8)$ Weisskopf units (W.u.) [16]. Further the $\gamma$ decay proceeds via a relatively prompt 137.7 keV $M1$ transition to the first isomeric state [17].

In order to gather more spectroscopic information on the $11/2^-$ isomeric state and on the evolution of the quenching factor, the $g$ factor of this isomeric state has been measured, results and interpretations are presented in the following.

## II. EXPERIMENTAL MEASUREMENTS

The experiment was performed at the tandem accelerator of the CEA Bruyères le Châtel, France. The $^{99}$Mo isotope was produced at different excited states [18] and spin-aligned [19] in a (d,p) reaction with a pulsed 6 MeV energy deuteron beam impinging on an highly enriched annealed $^{98}$Mo target. At the same time the target was used as a non-perturbative host. The $l = 5$ transitions were found to be strong [20], allowing sufficient production rate of the $J^\pi = 11/2^-$ state to be investigated. The spin-oriented ensemble of an isomeric state induces anisotropy in the $\gamma$-ray emission. The Time-Dependent Perturbed Angular Distribution (TDPAD) method was applied for the measurement of this anisotropy, leading to the $g$ factor determination of the metastable state $^{99\mathrm{m}2}$Mo, $E_x = 684.10$ keV and $J^\pi = 11/2^-$.

The TDPAD apparatus consisted of a crystal host, namely the $^{98}$Mo target, a dipole electromagnet, and $\gamma$-ray detectors. Under an external magnetic field $B_0$ perpendicular to the beam axis which corresponds to the spin-orientation axis, the spin precesses the ensemble with a Larmor frequency $\omega_L = -g\mu_\mathrm{N}B_0/\hbar$, where $g$ is the $g$ factor, $\mu_\mathrm{N}$ the nuclear magneton, and $\hbar$ the reduced Planck constant. The observation of the $\gamma$-ray anisotropy synchronized with the Larmor precession enables us to determine the $g$ factor. The delayed $\gamma$-rays from the decay of the isomeric state were observed with four high purity germanium detectors (HPGe) positioned in the horizontal plane at $\pm 135°$ and $\pm 45°$ with respect to the beam axis. As the $\gamma$-rays below 150 keV have a worse timing resolution, only the isomeric transition $E_\gamma = 448.6$ keV was used for the determination of the $g$ factor.

Angular distribution of the $\gamma$-ray anisotropy was evaluated with the standard $R(t)$-function giving the difference in the intensities between two detectors positioned at 90° with respect to each other as

$$R(t) = \frac{I(t,\theta) - I(t,\pi/2+\theta)}{I(t,\theta) + I(t,\pi/2+\theta)}, \tag{1}$$

where $I(t,\theta)$ is the $\gamma$-ray intensity at $t$-time for the detector positioned at an angle $\theta$. The $R(t)$ function allows to extract the Larmor frequency as

$$R(t) = \frac{3A_2B_2}{4 + A_2B_2}\cos[2(\theta - \omega_L t)], \tag{2}$$

where $A_2$ is the second-order angular distribution coefficient which depends on the multipolarity of the observed $\gamma$-transition and $B_2$ is the rank-two orientation tensor which depends on the spin orientation of the emitting state. Here, higher-order terms are neglected.

In order to include systematic errors, mainly due to the distribution of the magnetic field over the beam spot, we have measured the Larmor precession under identical conditions for the $^{66}$Cu isotope, using as target an annealed copper host. The $R(t)$ function of the $J^\pi = 6^-$ isomer having a known g factor of $g = +0.173(2)$ [21] has been done and $B_0 = 0.630(12)$ T was extracted for the applied magnetic field.

A typical delayed energy spectrum for the $^{98}$Mo(d,p)$^{99}$Mo reaction is presented in Fig. 1, where the isomeric transitions are clearly observed. The extracted half-life $T_{1/2} = 742(13)$ ns, shown in the inset of Fig. 1, is in good agreement with previous measurements [14, 16] leading to a more precise reduced transition probability $B(M2) = 0.104(3)$ W.u. value. Figure 2 represents the evaluated $R(t)$ function. Assuming a pure $M2$ transition for the $E = 448.6$ keV $\gamma$-ray, an amount of spin-alignment of the order of 15% is deduced. The $g$ factor of $^{99\mathrm{m}2}$Mo is determined to be $g_{\mathrm{exp.}} = -0.114(3)_{\mathrm{stat.}}(2)_{\mathrm{syst.}}$, thus, knowing the spin of this isomeric state to be $J = 11/2$, the magnetic moment of this isomeric state is calculated to be $\mu_{\mathrm{exp.}} = -0.627(20)$ $\mu_\mathrm{N}$. This result is far from the magnetic moments observed in the Cd chain and in $^{103}$Pd. In order to obtain a deeper insight into the structure of this state theoretical calculations were

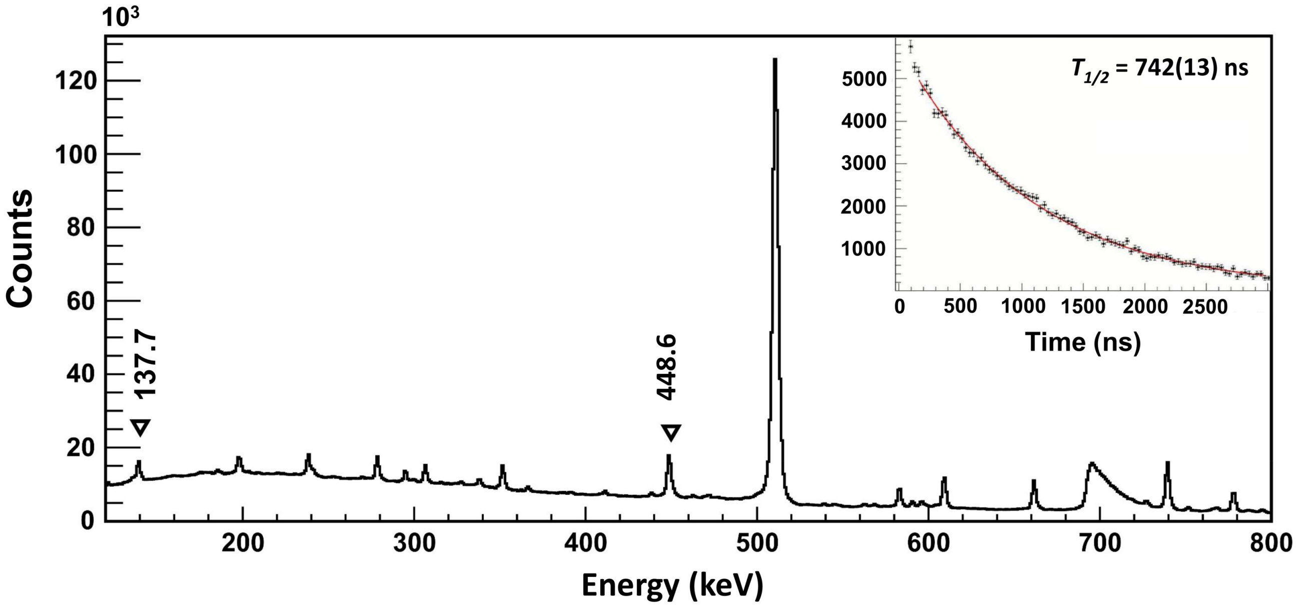


FIG. 1. Typical delayed $\gamma$-ray spectrum from the $^{98}$Mo(d,p)$^{99}$Mo reaction at 6 MeV. Observed transitions from the $^{99m2}$Mo are labeled with open triangles. The time spectrum of the 448.6 keV isomeric transition is shown as an inset.

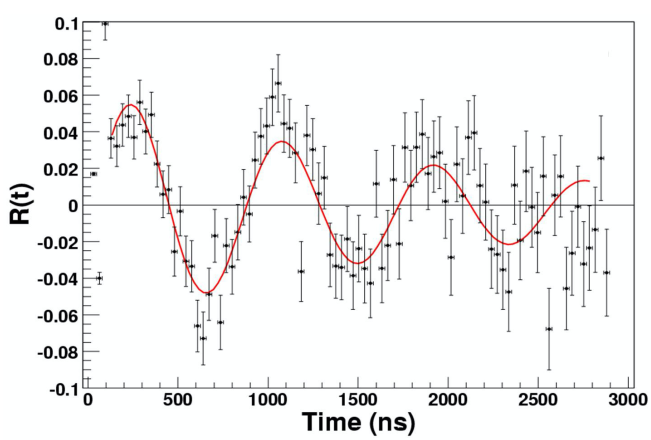


FIG. 2. $R(t)$ function associated with the 448.6 keV delayed $\gamma$-ray.

performed in the framework of an algebraic collective model as described in the following.

## III. THEORETICAL CALCULATIONS

We have investigated the nuclear structure properties of the $^{99}$Mo nucleus at low-excitation energies within the Interacting Boson-Fermion Model IBFM-1 [22, 23]. Of major interest in this investigation was to study the sensitivity of the nuclear magnetic moments to the single-particle orbital admixtures in the wave functions and the collectivity of different states, and how can one explain the large difference between the measured magnetic moment of the $11/2^-$ state of this nucleus, of $\mu_{\text{exp.}} = -0.627\ \mu_{\text{N}}$ and the Schmidt value for free neutron in the $h_{11/2}$ orbital, $\mu_{\text{free}}(\nu h_{11/2}) = -1.913\ \mu_{\text{N}}$.

The present IBFM-1 calculations are similar with those performed, e.g., for its neighbor isotope $^{97}$Mo [8] and for other nuclei in the same mass region that will be refered to later. $^{99}$Mo was regarded as an odd fermion (neutron hole) coupled to a $^{100}$Mo core nucleus that was described by the Interacting Boson Model IBM-1 [23, 24]. The odd fermion was allowed to occupy the single particle orbits from the 50 to 82 major shell, namely, $d_{5/2}$, $g_{7/2}$, $s_{1/2}$, $d_{3/2}$, and $h_{11/2}$. For the single-particle (s.p.) energies of these orbitals we started from the values of Reehal and Sorensen prescription [25], and modified especially those of the $g_{7/2}$ orbital, increased by about 0.6 MeV, and of the $s_{1/2}$ one, lowereded by about 1 MeV, such as to be able to describe the energies of the lowest states in this nucleus. Thus, the s.p. energies relative to that of the $d_{5/2}$ orbital were: 2.4 MeV ($g_{7/2}$), 1.1 MeV ($s_{1/2}$), 3.0 MeV ($d_{3/2}$), and 2.7 MeV ($h_{11/2}$), and their corresponding quasi-particle energies and orbital occupancies were calculated by BCS with a standard pairing gap of 1.5 MeV. Besides these values, and the IBM-1 core Hamiltonian parameters, there were the strengths of the boson-fermion interaction, which were chosen as $A_0 = -0.05$ MeV, $\Gamma_0 = 0.34$ MeV, and $\Lambda_0 = 1.30$ MeV$^2$ for the monopole, quadrupole, and exchange interactions, respectively [26]. These values were used to calculate both the positive- and negative-parity states.

The IBFM-1 calculations, in which one does not distinguish between neutron and proton bosons, were performed with the existing ODDA, PBEM, and SPEC programs [26], which calculate the energy levels, electromagnetic transition rates and moments, and one-neutron transfer spectroscopic factors, respectively. Figure 3

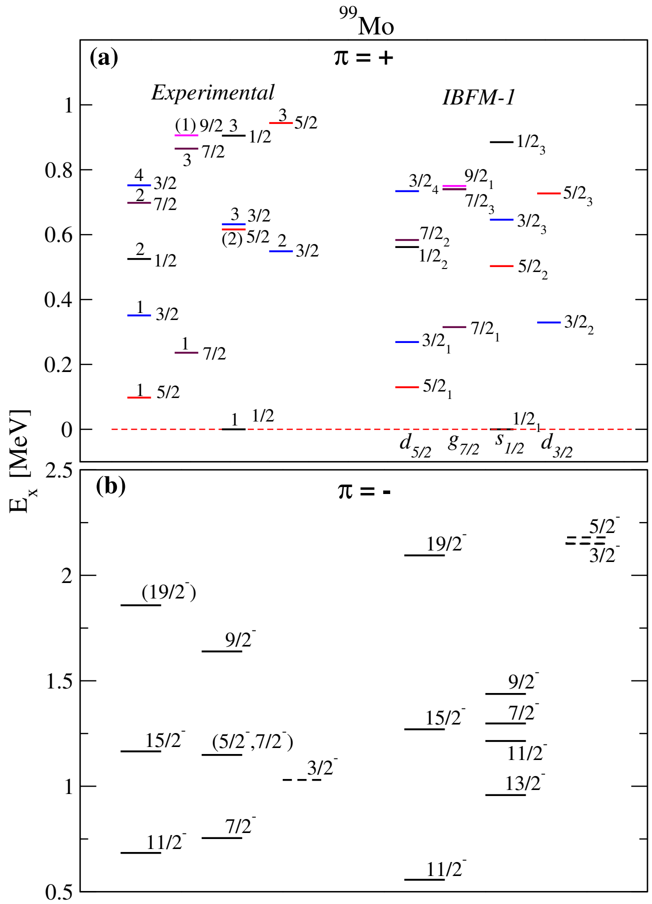


FIG. 3. Comparison between experimental levels and IBFM-1 calculated ones. The IBFM levels are arranged according to their dominant s.p. component of the wave-function. The experimental energy levels are labeled with the order number of the assigned calculated state of the same spin. See also Table I and text discussion. The experimental levels are from Ref. [17].

shows a comparison of the experimental low-energy level scheme with positive-parity states up to about 1 MeV, and negative-parity states up to about 2 MeV [17], with the results of these calculations. The calculated positive-parity energy levels are arranged and labeled according to the dominant s.p. orbital in their wave-functions.

The correspondence between the calculated and experimental levels was made on the basis of all known spectroscopic properties: energy levels, electromagnetic decay mode (branching ratios), absolute electromagnetic decay rates, spectroscopic factors for the one-neutron transfer reaction, and magnetic and quadrupole moments. In Fig. 3, the experimental levels of positive-parity of each spin were labeled with the level number of the assigned calculated level of the same spin. For the negative parity states, the favored $11/2^-$, $15/2^-$, $19/2^-$ sequence is reasonably well reproduced, although with a slightly smaller moment of inertia than the experimental one. The lowest spin members of the calculated multiplet $2^+_{core} \times h_{11/2}$, $7/2^-$ and $9/2^-$, may correspond to known experimental states. The experimental low-lying $3/2^-$ and eventually $(5/2^-)$ states are not accounted for by the calculations, as the first calculated states with these spin values are rather high in energy.

Table I shows the experimental and calculated spectroscopic properties, some of them being discussed later in more detail.

TABLE I: Comparison of different experimental and calculated (IBFM-1) spectroscopic properties for the low-lying states of $^{99}$Mo below 700 keV excitation energy. For the level within parentheses the assignment of the calculated level is only tentative. $C^2S$ are the spectroscopic factors for the neutron pickup reactions (p,d) and (d,t). A value $GS = -1.721\ \mu_{\rm N}$ (quenching factor of 0.45) was used. The experimental data are from Ref. [17].

| $J_i^\pi$ | E$_x$ [keV] | $J_f^\pi$ | $\mu$ [$\mu_N$] exp. | calc. | $Q$ [e·b] calc. | $C^2S$ exp. | calc. | Branch exp. | calc. | $B(E2)$ [W.u.] exp. | calc. | $B(M1)$ [W.u.] exp. | calc. |
|---|---|---|---|---|---|---|---|---|---|---|---|---|---|
| $1/2^+_1$ | 0 | | ±0.375(3) | -0.719 | - | (0.30) | 0.51 | | | | | | |
| $5/2^+_1$ | 97.8 | | -0.775(5) | -0.769 | 0.514 | 1.84 | 3.47 | | | | | | |
| | | $1/2^+_1$ | | | | | | 100 | 100 | 0.0650(10) | 0.68 | | |
| $7/2^+_1$ | 235.5 | | – | 0.862 | -0.827 | 1.39 | 0.31 | | | | | | |
| | | $5/2^+_1$ | | | | | | 100 | 100 | | | 8.8(16) | 0.085 |
| $3/2^+_1$ | 351.2 | | – | 0.189 | -0.252 | 0.06 | 0.02 | | | | | | |
| | | $5/2^+_1$ | | | | | | 100 | 100 | | | 3.3(25) | 3.5 |
| | | $1/2^+_1$ | | | | | | 75 | 91 | | | 0.9(7) | 0.5 |
| $1/2^+_2$ | 525.2 | | – | -0.815 | - | $\sim 0$ | 0.003 | | | | | | |
| | | $3/2^+_1$ | | | | | | 22 | 38 | | | | |
| | | $5/2^+_1$ | | | | | | 52 | 78 | | | | |
| | | $1/2^+_1$ | | | | | | 100 | 100 | | | | |

| | | | | | | | | | | | | | |
|---|---|---|---|---|---|---|---|---|---|---|---|---|---|
| $3/2^+_2$ | 548.7 | | – | -0.016 | -0.295 | 0.33 | 0.03 | | | | | | |
| | | $3/2^+_1$ | | | | | | 14 | 3 | | 0.4 | | 37 |
| | | $5/2^+_1$ | | | | | | 100 | 100 | $< 3.9$ | 12.6 | $> 0.83$ | 104 |
| | | $1/2^+_1$ | | | | | | 29 | 1 | $\sim 1.1$ | 1.38 | $\sim$0.54 | 0.08 |
| $(5/2^+_2)$ | 615.0 | | – | 0.196 | 0.237 | 0.24 | 0.25 | | | | | | |
| | | $3/2^+_1$ | | | | | | 100 | 45 | | | | |
| | | $7/2^+_1$ | | | | | | 24 | 1 | | | | |
| | | $5/2^+_1$ | | | | | | - | 23 | | | | |
| | | $1/2^+_1$ | | | | | | - | 100 | | | | |
| $3/2^+_3$ | 631.8 | | – | 0.919 | 0.179 | – | $\sim 0$ | | | | | | |
| | | $3/2^+_1$ | | | | | | 16 | 12 | | | | |
| | | $5/2^+_1$ | | | | | | 42 | 4 | | | | |
| | | $1/2^+_1$ | | | | | | 100 | 100 | | | | |
| $7/2^+_2$ | 698.1 | | – | 0.381 | 0.299 | | | | | | | | |
| | | $7/2^+_1$ | | | | | | 21 | 4 | | | | |
| | | $5/2^+_1$ | | | | | | 100 | 100 | | | | |
| $11/2^-_1$ | 684.1 | | -0.627(16) | -0.626 | -1.380 | 0.50 | 0.26 | | | | | | |
| | | $7/2^+_1$ | | | | | | 100 | | M2: 0.103(8) | | | |

TABLE II. Wave-function composition of some low-lying positive-parity states.

| J$^\pi$ | Exp. $E_x$ (keV) | Calc. $E_x$ (keV) | W-f. composition (%) $d_{5/2}$ | $g_{7/2}$ | $s_{1/2}$ | $d_{3/2}$ | $h_{11/2}$ |
|---|---|---|---|---|---|---|---|
| $\frac{1}{2}^+$ | 0.0 | 0.0 | 2.4 | 2.7 | 80.7 | 14.2 | 0 |
| | 525.2 | 561.7 | 89.7 | 0.6 | 7.6 | 2.1 | 0 |
| $\frac{3}{2}^+$ | 351.2 | 269.1 | 59.0 | 9.8 | 17.3 | 13.8 | 0 |
| | 548.7 | 329.3 | 28.3 | 28.2 | 0.3 | 43.2 | 0 |
| | 631.8 | 646.0 | 28.8 | 10.7 | 41.3 | 19.2 | 0 |
| $\frac{5}{2}^+$ | 97.8 | 129.7 | 96.5 | 0.8 | 1.5 | 1.2 | 0 |
| | (615.0) | 503.0 | 13.7 | 4.5 | 69.0 | 12.8 | 0 |
| $\frac{7}{2}^+$ | 235.5 | 314.6 | 0.2 | 88.7 | 0.2 | 10.9 | 0 |
| | 698.1 | 583.5 | 87.3 | 4.4 | 0.2 | 8.1 | 0 |
| $\frac{11}{2}^-$ | 684.1 | 558.3 | 0 | 0 | 0 | 0 | 100 |

Table II displays the composition of the wave-functions of the lowest-lying levels. From Fig. 3 and Table I, one sees that the calculated structures explain reasonably well the known spectroscopic properties of the positive-parity states, and notably, the isomeric character of first states of spin 3/2, 5/2, and 7/2, as well as the three measured magnetic moments. The negative-parity states within this approach are entirely due to the intruder orbital $h_{11/2}$, which does not mix with the positive-parity orbitals.

Let us discuss now the quantities/parameters that determine the electromagnetic transition operators. For the $E2$ transitions, the quadrupole operator was mainly determined by the one that describes the $^{100}$Mo core, to which the odd-fermion contribution was added, with a fermionic effective charge taken equal to the bosonic one (0.103 e·b). For the $M1$ transition operator, we used the simplest form [26]:

$$T(M1) = \sqrt{\frac{90}{4\pi}} GD (d^\dagger \times \tilde{d})^{(1)} + \sum_{j \leq j'} \frac{g^1_{jj'}}{1+\delta_{jj'}} \{(a_j \times \tilde{a}_{j'})^{(1)}$$

$$+(-1)^{(j-j')}(a_{j'} \times \tilde{a}_j)^{(1)}\}$$

with

$$g^1_{j,j'} = -\frac{1}{\sqrt{3}} < l_j \frac{1}{2} j \| GL\vec{l} + GS\vec{s} \| l_{j'} \frac{1}{2} j' > .$$

Here, $GD$ denotes the effective d-boson $g$ factor, and $GL$ and $GS$ are the effective single-particle angular momentum and spin $g$ factors of the fermion.

In our case, $GD$ was taken as 0.47 $\mu_N$, as determined from the $g$ factor of the $2^+_1$ state of the core [27]. Since the odd fermion is a neutron, $GL = 0$, while $GS$ is determined from the experimental data. For a free neutron, $GS = -3.826$ $\mu_N$. However, in theoretical calculations it was found that in order to describe the experimental data, $M1$ transition strengths and magnetic moments, one must use an effective $GS$ value smaller than the free value one, by multiplying the latter with a quenching factor, smaller than 1. In most of the IBFM calculations one has taken a quenching factor of 0.7, leading to $GS = -2.678$ $\mu_N$, which became a kind of common rule. By using this customary value the calculated magnetic moment of the $11/2^-$ state was around a value of $-1.2$ $\mu_N$, almost the double of the measured $-0.627$ $\mu_N$.

Initially, this large difference was attributed to the possibility that the $11/2^-$ level is not a pure $\nu h_{11/2}$ state. Thus, we thought of two possibilities. The first one was to test the effect of including other negative-parity orbitals in the calculation of the negative-parity states. To this end, we have included the $f_{7/2}$ and $h_{9/2}$ orbitals from the next major shell, above the $N = 82$ gap. Because these orbitals are rather distant, their influence was very small, resulting to a few percent contribution in the wave-function and very small changes of the magnetic moment of the $11/2^-$ state. The second possibility was that the $11/2^-$ state has, besides the single-particle $h_{11/2}$ dominant configuration, some component resulting either from coupling the positive-parity orbitals $d_{5/2}$ or $g_{7/2}$ to the $3^-$ state of the core at 1.908 MeV, or from couplings of the four positive-parity orbitals to the $4^-$, $5^-$ states resulting from proton excitations like $(p^{-1}_{1/2}g^{1}_{9/2})$. However, both these cases are not energetically favoured, therefore their contributions are not expected to be large.

The only possibility to improve the description of the magnetic moment within the present IBFM-1 approach, in which the $11/2^-$ has a pure $h_{11/2}$ single-particle character, was to vary the quenching of the free neutron spin $g$ factor. It was found that the magnetic moments are very sensitive to this quantity, and that for a quenching factor of 0.45 ($GS = -1.721\ \mu_{\rm N}$), one can match exactly the experimental magnetic moment of the $11/2^-$ state, as shown in the Table I. An indication of the fact that this is more than a simple "normalisation" of a parameter to just one experimental value, was that a similar improvement was simultaneously obtained for the magnetic moment of the $5/2^+_1$ state, and some improvement took place also for the magnetic moment of the $1/2^+$ ground state. With the customary quenching of 0.70, the calculated values were around $-1.2\ \mu_{\rm N}$ for both these states, compared to the experimental ones of $\pm 0.375\ \mu_{\rm N}$ and $-0.775\ \mu_{\rm N}$, respectively, see Table I. For spins 1/2, the wave function is usually highly fragmented and the contribution of every 1/2 state may not be accurately described. Thus, the calculated magnetic moments, which do reflect the wave function, may not be well established. In our case, the magnetic moment of the $1/2^+$ ground state, calculated for the quenching of 0.45, is still about twice larger than the experimental value. However, we have a serious reason to assume that the neutron spin $g$ factor quenching in this nucleus must be of about 0.45. This prompted us to investigate the role of the quenching factor in similar IBFM-1 studies of other nuclei from the same mass region.

## IV. NEUTRON SPIN $g$ FACTOR QUENCHING IN MASS $\sim 100$ NUCLEI

The discussion above questions the "customary" prescription of a quenching factor of 0.70 in the IBFM-1 calculations at least for the $^{99}$Mo nucleus. Is that a singular case? Fortunately, we have found a number of neutron-odd nuclei in the vicinity of $^{99}$Mo, for which multi-shell IBFM-1 descriptions were given for the same 50 - 82 single particle space, so that we were able to investigate the effect of changing the quenching factor. Similarly to the case of $^{99}$Mo, the magnetic moments were found to be rather sensitive to the value of the quenching factor, while the $M1$ transition rates were much less sensitive.

These nuclei are the following: $^{99}$Zr [28, 29], $^{97}$Mo [8], the Ru isotopes 99 to 105 [30], and $^{113}$Cd [31]. For all these nuclei the published IBFM-1 calculations were made with the prescription $GS = -2.678\ \mu_{\rm N}$, that is, with a quenching factor of 0.7. The predictions of all these calculations were compared with $M1$ transition probabilities, and sometimes also with existing magnetic moments, providing a qualitative agreement with the experimental values. Taking advantage of the known Hamiltonian and transition operators parameters, we were able to easily re-calculate these cases and study the influence of $GS$ on the magnetic moments. Figure 4 displays a comparison of experimentally measured magnetic moments for states of different spins in these nuclei, with IBFM-1 calculated values for different quenching factors of $GS$, between 0.70 and 0.45. In the case of $^{99}$Zr, where one can see that a compromise value of the quenching factor of $\approx 0.5$ provides an optimum description of all three known magnetic moments, it was checked that the $M1$ transition rates were rather insensitive to the variation of $GS$ and thus the conclusions of refs. [28, 29] remain unchanged. By examining Fig. 4 one can see that from a number of fifteen experimental magnetic moments, twelve are best described for quenching factors in the range 0.45 to 0.55. In another systematic IBFM-1 study of the $^{125-131}$Xe and $^{123-131}$Te isotopes [32], within the same s.p. model space, a value of 0.4 was chosen for the quenching factor, on the basis of the analysis of many experimental spectroscopic properties. Therefore, one may conclude that for odd-neutron nuclei in the mass $A \sim 100$ region, IBFM-1 calculations with the odd nucleon occupying the orbitals available within the 50 to 82 major shell, a quenching of the free neutron spin $g$ factor of about 0.5 offers the best description of the experimental data, in particular of the magnetic moments which are rather sensitive to this quantity.

Effective values for the neutron spin $g$ factor, therefore the use of a quenching factor, are also common to other theoretical model approaches, including the shell model. The main reason of this quenching is the inadequacy of the lowest-order shell-model wavefunctions [33]. Calculations of the core polarization and meson-exchange current effects lead to equivalent effective one-body $M1$ operators [33]. The completeness of the shell-model space used and its associated effective interaction determine the effective operator, therefore the quenching of the free nucleon $g$ factor. Thus, in calculations for the $sd$ shell [34] and $fp$ shell [35] nuclei the use of the free-nucleon $g$ factors provided a good description of the experimental data. In contrast, in the $f_5pg_9$ shell, corresponding to nuclei between $^{57}$Ni and $^{96}$Pd, a good description of the magnetic moments definitely required a quenching factor of 0.7, which reflects the incompleteness of the model space with respect to the spin-orbit partners, that is, the $^{56}$Ni core is not $LS$ closed [36]. As an example, the main reason for the deviation of the magnetic moment of the isomeric state $9/2^+$ in $^{65}$Ni from the Schmidt value of the $\nu g_{9/2}$ orbital was found in the contributions of the proton excitations from the $f_{7/2}$ orbital across the $Z = 28$ gap [37].

In the higher mass $^{126}$Sn nucleus [38], a smaller neutron quenching factor of 0.65 was used, and the main core polarization configurations for the $M1$ operator were found the neutron $(h^{-1}_{11/2}h_{9/2})$ and the proton $(g^{-1}_{9/2}g_{7/2})$ cross-shell excitations.

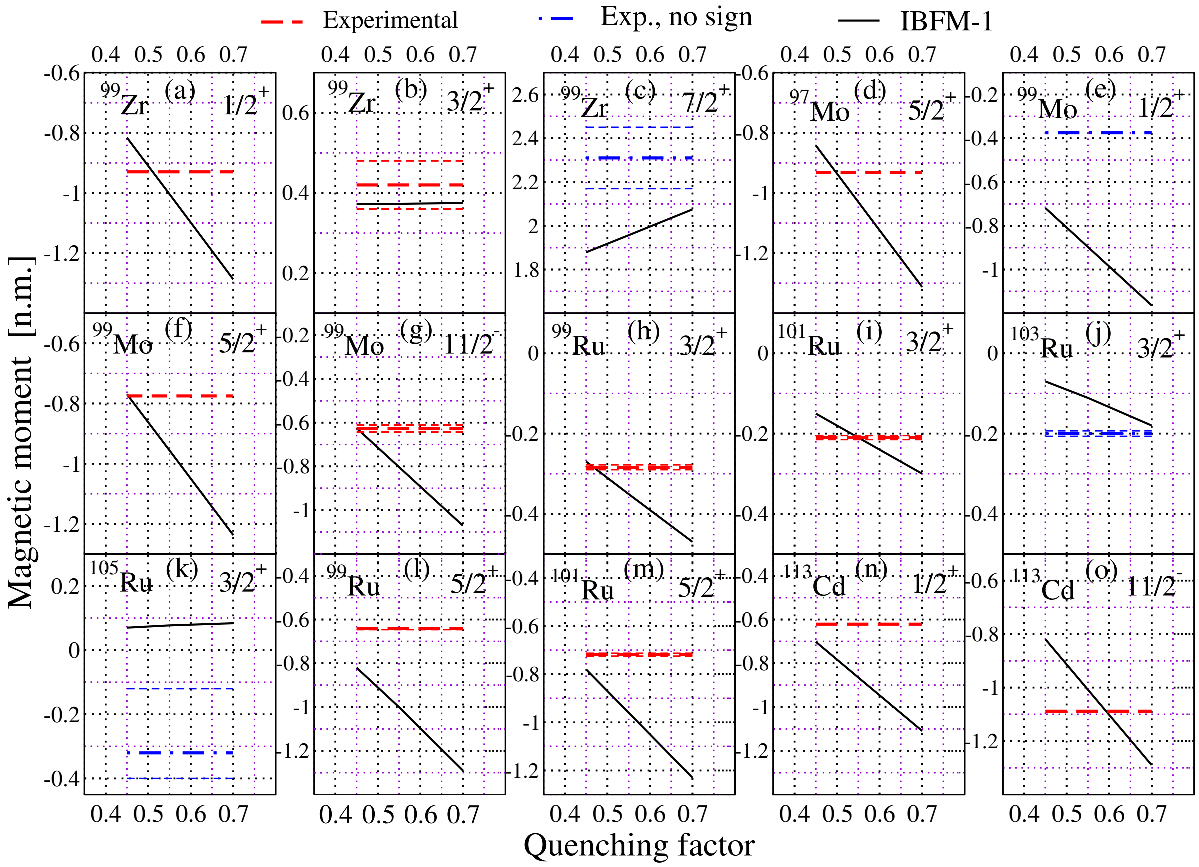


FIG. 4. Comparison between experimental magnetic moments and IBFM-1 values calculated for different quenching factors for the neutron spin $g$ factor. The experimental values are represented by horizontal lines: dashed (red) for the values determined with sign, dash-dotted (blue) for those determined without sign. For the values determined with larger errors, the error bars are visible too. The calculated values are the black continuous lines. The experimental values were taken from [1]. See text for the articles with IBFM-1 approaches of the nuclei from this figure.

## V. CONCLUSIONS

In summary, the $11/2^-$ isomeric state of $^{99}$Mo was carefully investigated via the $g$ factor measurement. The reported magnetic moment $\mu_{\mathrm{exp.}} = -0.627(20)\ \mu_{\mathrm{N}}$ shows a value that is quite far from the one expected for a pure single-particle $\nu h_{11/2}$ configuration. To shed light on the configuration of this measured isomeric state multi-shell Interacting Boson-Fermion Model IBFM-1 calculations were performed, with the odd nucleon allowed to occupy the orbitals from the $N = 50 - 82$ shell. Spectroscopic properties like level energies, electromagnetic decays, and $g$ factors of the low-lying states of both parities were calculated and compared with experimental values. Experimental $g$ factors of three states in this nucleus, including that of the pure $\nu h_{11/2}$ $11/2^-$ state, are well reproduced by the model calculations using a quenching factor of 0.45 for the free neutron spin $g$ factor. The need of such a low value of the quenching factor, compared to the usually recommended value of 0.70, was confirmed by an examination of an enlarged set of nuclei from the $A \approx 100$ region for which IBFM-1 parametrizations in the same shell orbit space were known. The description of most of the known magnetic moments in these nuclei clearly asked for a quenching of the free neutron spin $g$ factor of about 0.5. It would be interesting to investigate this quenching in the same nuclei with shell-model calculations with different truncation schemes.

## VI. ACKNOWLEDGMENTS

We are greatful to G. Alloy, J.J. Baldys, F. Goffard, and M. Reverberi for providing us the beam. We would like to thank Frederico Garrido from IJClab for annealing the enriched isotope target.

[1] N. J. Stone, INDC(NDS)-0794 (2019).

[2] T. Schmidt, Z. Phys. **106**, 58 (1937).

[3] D. T. Yordanov, D. L. Balabanski, J. Bieron, M. L. Bissell, K. Blaum, I. Budincevic, S. Fritzsche, N. Frommgen, G. Georgiev, Ch. Geppert, M. Hammen, M. Kowalska, K. Kreim, A. Krieger, R. Neugart, W. Nortershauser, J. Papuga, S. Schmidt, Phys.Rev.Lett. **110**, 192501 (2013).

[4] D. Riegel, N. Brauer, F. Dimmling, B. Focke, K. Nishiyama, Phys.Lett. **46B**, 170 (1973).

[5] L. G. Kostova, W. Andrejtseheff, L. K. Kostov, L. Funke, E. Will, and A. I. Vdovin, Z. Phys. A **342**, 145 (1992).

[6] P. H. Regan, C. W. Beausang, N. V. Zamfir, R. F. Casten, J.-Y. Zhang, A. D. Yamamoto, M. A. Caprio, G. Gurdal, A. A. Hecht, C. Hutter, R. Krucken, S. D. Langdown, D. A. Meyer, J. J. Ressler, Phys.Rev.Lett. **90**, 152502 (2003).

[7] Y. H. Zhang, M. Hasegawa, W. T. Guo, M. L. Liu, X. H. Zhou, G. de Angelis, T. M. Axiotis, A. Gadea, N. Marginean, Martinez, D. R. Napoli, C. Rusu, Zs. Podolyak, C. Ur, D. Bazzacco, F. Brandolini, S. Lunardi, S. M. Lenzi, R. Menegazzo, R. Schwengner, A. Gargano, W. von Oertzen, S. Tazaki, Phys.Rev. C **79**, 044316 (2009).

[8] D. Bucurescu, Ghe. Căta-Danil, I. Căta-Danil,, M. Ivaşcu, N. Mărginean, and C.A. Ur, Phys. Rev. C **63**, 014306 (2000).

[9] P. H. Regan, A. D. Yamamoto, F. R. Xu, C. Y. Wu, A. O. Macchiavelli, D. Cline, J. F. Smith, S. J. Freeman, J. J. Valiente-Dobón, K. Andgren, R. S. Chakrawarthy, M. Cromaz, P. Fallon, W. Gelletly, A. Gorgen, A. Hayes, H. Hua, S. D. Langdown, I-Y. Lee, C. J. Pearson, Zs. Podolyák, R. Teng, and C. Wheldon, Phys. Rev. C **68**, 044313 (2003).

[10] J. Timar, J. Gizon, A. Gizon, D. Sohler, B. M. Nyako, L. Zolnai, A. J. Boston, D. T. Joss, E. S. Paul, A. T. Semple, C. M. Parry, I. Ragnarsson, Phys.Rev. C **62**, 044317 (2000).

[11] A. D. Yamamoto, P. H. Regan, C. W. Beausang, F. R. Xu, M. A. Caprio, R. F. Casten, G. Gurdal, A. A. Hecht, C. Hutter, R. Krucken, S. D. Langdown, D. Meyer, J. J. Ressler, N. V. Zamfir, Phys.Rev. C **66**, 024302 (2002).

[12] N. Fotiades, J. A. Cizewski, D. P. McNabb, K. Y. Ding, D. E. Archer, J. A. Becker, L. A. Bernstein, K. Hauschild, W. Younes, R. M. Clark, P. Fallon, I. Y. Lee, A. O. Macchiavelli, R. W. MacLeod, Phys.Rev. C **58**, 1997 (1998).

[13] Robert B. Duffield and Stanley H. Vegors, Jr., Phys.Rev. **112**, 1958 (1958).

[14] W. Dietrich, G. C. Madueme, L. Westerberg, A. Backlin, Phys.Scr. **12**, 271 (1975).

[15] J. Dubuc, G. Kajrys, P. Larivière, S. Pilotte, W. Del Bianco, and S. Monaro, Phys. Rev. C **37**, 954 (1988).

[16] H.Bartsch, K.Huber, U.Kneissl, H.Krieger, Z.Phys. A **285**, 273 (1978).

[17] E. Browne and J.K. Tuli, Nucl. Data Sheets **145**, 25 (2017).

[18] J. B. Moorhead, R. A. Moyer, Phys.Rev. 184, 1205 (1969).

[19] T. V. Ragland, R. J. Mitchell, R. P. Scharenberg, R. E. Holland, and F. J. Lynch, Phys. Rev. C **18**, 2494 (1978).

[20] W. Booth, S. M. Dalgliesh, K. C. McLean, R. N. Glover, F. R. Hudson, Phys.Letters **30B**, 335 (1969).

[21] J. Bleck, R. Butt, K. H. Lindenberger, W. Ribbe, W. Zeitz, Nucl.Phys. A **197**, 620 (1972).

[22] F. Iachello and O. Scholten, Phys. Rev. Lett. **43**, 679 (1979).

[23] F. Iachello and P. van Isacker, *The Interacting Boson-Fermion Model*, Cambridge Monographs on Mathematical Physics (Cambridge University Press, Cambridge, 1991).

[24] F. Iachello and A. Arima, Phys. Lett. B **53**, 309 (1974); Phys. Rev. Lett. **35**, 1069 (1975).

[25] B.S. Reehal and R.A. Sorensen, Phys. Rev. C **2**, 819 (1970).

[26] O. Scholten, computer codes ODDA and PBEM, KVI Internal Report no. 252, a982; computer code SPEC (unpublished).

[27] Balraj Singh, Nucl. Data Sheets **109**, 297 (2008).

[28] P. Spagnoletti, G. Simpson, S. Kisyov, D. Bucurescu, J.-M. Regis, N. Saed-Samii, A. Blanc, M. Jentschel, U. Köster, P. Mutti, T. Soldner, G. de France, C.A. Ur, W. Urban, A.M. Brucem C. Bernards, F. Drouet, L.M. Fraile, L.P. Gaffney, D.G. Ghiţă, S. Ilieva, J. Jolie, W. Korten, T. Kröll, S. Lalkovski, C. Larijarni, R. Lică, H. Mach N. Mărginean, V. Paziy, Zs. Podolyak, P.H. Regan, M. Scheck, J.F. Smith, G. Thiamova, C. Townsley, A. Vancraeyenest, V/ Vedia, N. Warr, V. Werner, and M. Zieli nska, Phys. Rev. C **100**, 014311 (2019).

[29] F. Boulay, G.S. Simpson, Y. Ichikawa, S. Kisyov, D. Bucurescu, A. Takamine, D.S. Ahn, K. Asahi, H. Baba, D.L. Balabanski, T. Egami, T. Fujita, N. Fukuda, C. Funayama, T. Furukawa, G. Georgiev, A. Gladkov, M. Hass, K. Imamura, N. Inabe, Y. Ishibashi, T. Kawaguchi, T. Kawamura, W. Kim, Y. Kobayashi, S. Kojima, A. Kusoglu, R. Lozeva, S. Momiyama, I. Mukul, M. Niikura, H. Nishibata, T. Nishizaka, A. Odahara, Y. Ohtomo, D. Ralet, T. Sato, Y. Shimizu, T. Sumikama, H. Suzuki, H. Takeda, L.C. Tao, Y. Togano, D. Tominaga, H. Ueno, H. Yamazaki, X.F. Yang, and J.M. Daugas, Phys. Rev. Lett. **124**, 112501 (2020).

[30] S. Kisyov, D. Bucurescu, J. Jolie, and S. Lalkovski, Phys. Rev. C **93**, 044308 (2016).

[31] D. Bucurescu, Y. Eisermann, G. Graw, R. Hertenberger, H.-F. Wirth, and Yu.V. Ponomarev, Nucl. Phys. A **756**, 54 (2005).

[32] S. Abu-Musleh, H.M. Abu-Zeid, and O. Scholten, Nucl. Phys. A **927**, 91 (2014).

[33] I.S. Towner, Phys. Rep. **155**, 263 (1987).

[34] B.A. Brown, Prog. Part. Nucl. Phys. **47**, 517 (2001).

[35] M. Honma, T. Otsuka, B.A. Brown, and T. Mizusaki, Phys. Rev. C **69**, 034335 (2004).

[36] M. Honma, T. Otsuka, T. Mizusaki, and M. Hjorth-Jensen, Phys. Rev. C **80**, 064323 (2009).

[37] G. Georgiev, I. Matea, D.L. Balabanski, J.M. Daugas, F. de Oliveira Santos, S. Franchoo, F. Ibrahim, F. Le Blanc, M. Lewitowicz, G. Lo Bianco, S. Lukyanov, V. Meot, P. Morel, G. Neyens, Yu.E. Penionzhkevich, A. SaltarellI, O. Sorlin, M. Stanoiu, M. Tarisien, N. Vermeulen, D. Verney, and D. Yordanov, Eur. Phys. J. A **30**, 351 (2006).

[38] G. Ilie, G. Neyens, G.S. Simpson, J. Jolie, A. Blazhev, H. Grawe, R.L. Lozeva, N. Vermeulen, L. Atanasova, D.L. Balabanski, H. Becker, P. Bednarczyk, C. Brandau, L. Caceres, S.K. Chamoli, J.M. Daugas, P. Doornenbal, J. Gerl, M.Górska, J. Grebosz, M. Hass, M. Ionescu-Bujor, A. Jungclaus, M. Kmiecik, I. Kojouharov, N. Kurz, A. Maj, S. Mallion, O. Perru,

M. Pfútzner, Zs. Podolyak, W. Prokopowicz, M. De Rydt, T.R. Saito, H. Schaffner, K. Turzó, J. Walker, E. Werner-Malento, H.J. Wollersheim, Phys. Lett. B **687**, 305 (2010).